Ceramics International xxx (xxxx) xxx–xxx

Contents lists available at ScienceDirect

Ceramics International

journal homepage: www.elsevier.com/locate/ceramint

Lead-free ferroelectric $Na_{1-x}Sr_x$ $(Sn_{0.25}Ti_{0.75})_xNb_{1-x}O_3$ system ($0.1 \le x \le 0.4$) XRD, dielectric, and Raman properties

S. Aydi*, A. Amouri, S. Chkoundali, A. Aydi

Laboratoire des Matériaux Multifonctionnels et Applications (LMMA), et Applications, Université de Sfax, Faculté des Sciences de Sfax (FSS), Route de Soukra, km3,5, B.P.1171, 3000 Sfax, Tunisia

ARTICLE INFO

Keywords:
Antiferroelectric
Ferroelectric
Relaxor
Raman
Hysteresis, Stable

ABSTRACT

$Na_{1-x}Sr_x(Sn_{0.25}Ti_{0.75})_xNb_{1-x}O_3$ (SNSTNx) ceramics with composition ($0.1 \le x \le 0.4$) were synthesized by the conventional solid-state method. The purity, microstructure, dielectric, ferroelectric and Raman features were sought. This study demonstrated that antiferroelectricity can be stabilized in $NaNbO_3$-based ceramics by lowering the tolerance factor. This compound exhibited a single phase of perovskite without impurity with tetragonal symmetry (*P4mm*). Micro structural investigations, using both XRD and SEM, indicated an enhancement of antiferroelectric super lattice peaks with $SrSnO_3$ and $SrTiO_3$. The dielectric study showed that our new ceramics had better characteristics than pure $NaNbO_3$ and the relaxor behavior demonstrated the SNSTNx candidacy for use in several industrial applications. The ferroelectric behavior revealed that only ferroelectric domains existed in the prepared ceramic. In contrast, $NaNbO_3$ displayed the coexistence of antiferroelectric and ferroelectric domains. The Raman spectra of SNSTNx as a function of composition and temperature were also in favor of our dielectric results.

1. Introduction

Although Sodium Niobate $NaNbO_3$ (NN) has been investigated for several decades, the crystal structure and electrical properties are still debatable [1–5], namely XRD of NN poster and antiferroelectric (AFE) properties at room temperature with orthorhombic structure and space group Pbma [6]. Below 913 K, a whole series of structural phase transitions was found and at least six more phases were identified. The successive phases, labeled T2, T_1, S, R and P, are of orthorhombic symmetry, except T_2 which is tetragonal [7]. The dielectric behavior of NN sample has been widely investigated. It exhibits a phase transition at T_C around 913 K with a maxim real permittivity of ε'_{rmax} 1750 at T_C [8]. It is antiferroelectric at room temperature [9,10]. It seems that the confusion stems from the appearance of the polarization vs. electric field hysteresis loops. However, for high quality NN single crystal double hysteresis loops, antiferroelectric characteristics have been reported at room temperature [11,12]. Under an electric applied field perpendicular to the orthorhombic c axis during initial cycles, a square loop revealing ferroelectric (FE) behavior was reported [13]. On the other hand, for polycrystalline NN ceramics, square polarization hysteresis loops were observed at room temperature [14]. NN polycrystalline ceramic was also reported to be antiferroelectric at room temperature and, when exposed to a strong electric field, it transforms into a metastable ferroelectric phase [15]. Considering this ferroelectric or antiferroelectric phase instability, it is of great interest to discover ceramics with an electric stable phase.

The Strontium stannate $SrSnO_3$ has long attracted interest since structural studies by Megaw [16]. Structural transition investigation has not been limited to XRD [17,18], but it has been exhaustively investigated by neutron diffraction [19], ab initio DFT calculations [20] and several characterization techniques [21,22]. At room temperature, it exhibits a Pbnm orthorhombic structure with a small distortion from the cubic ones. The $SrTiO_3$ perovskite structure has a cubic symmetry at room temperature. But it possesses two phase transitions at low temperature. At firstly from orthorhombic to quadratic, then from quadratic to cubic at 65 K and 110 K [23].

This work aims at reaching a new lead-free $Na_{1-x}Sr_x$-$(Sn_{0.25}Ti_{0.75})_xNb_{1-x}O_3$ (SNSTNx) ferroelectric ceramic, as a result of both the substitution of Na^+ by Sr^{2+} and Nb^{5+} by (Ti^{4+},Sn^{4+}) in A and B sites, respectively. By increasing substitution, the FE phase is progressively favored and stabilized at the expense of AFE behavior of undoped NN sample. In this respect, a previous study [24] of NN system demonstrated that the lowering of both values of Goldsmiths tolerance factor (t) and average electro negativity (x) allowed stabilizing the competition between FE and AFE coexistence phases and favored AFE ones. Our SNSTNx ceramic with x = 0.1; 0.2; 0.3 and 0.4 compositions,

* Corresponding author.
E-mail address: aaydisamia@yahoo.fr (S. Aydi).

http://dx.doi.org/10.1016/j.ceramint.2017.06.076
Received 31 May 2017; Received in revised form 11 June 2017; Accepted 12 June 2017

synthesized by conventional solid-state reaction, showed an increase for t from 0.899 to 1.05 for x = 0.1 and from 0.9141 to 1.2 for x = 0.2. Thus, such behaviors predict a stabilized FE phase and the enhancement of electrical properties. Our samples were characterized by XRD; SEM equipped with an energy dispersive X-ray (EDX) detector, dielectric, ferroelectric hysteresis loops and Raman measurements.

2. Experimental techniques

The $Na_{1-x}Sr_x(Sn_{0.25}Ti_{0.75})_xNb_{1-x}O_3$ ($0.1 \le x \le 0.4$) ceramics were prepared by a conventional solid-state reaction method. The precursors (Aldrich with 99.9 of purity): Strontium carbonate ($SrCO_3$), Sodium carbonate (Na_2CO_3), Etain oxide (SnO_2), Titanium oxide (TiO_2) and Niobium oxide (Nb_2O_5) were carefully weighed in stoichiometric ratio and then wet mixed in an agate mortar for 2 h (h). Samples were dried, then pressed into discs of 13 mm in diameter, 10 mm in thickness and subsequently calcined at 1523 K for 12 h in air. The calcined powders were re-milled for 1 h, then shaped into pellets of 8 mm in diameter by uniaxial pressing of 100 MPa for one minute and underwent a second heat treatment. Our samples were sintered at a high temperature range of 1623 K for 2 h in air. The densities of all samples analyzed by Archimedes method were found to be higher than 96%. The chemical elements in the different compositions were analyzed qualitatively and semi-quantitatively using a SEM model JEOL 6360 A, equipped with an EDX detector. The SEM was employed to observe and distinguish the different chemical elemental compositions. Samples were observed in the low-vacuum secondary mode under a field of 15 kV and with a 30-nm resolution at an accelerating voltage of 50 kV. Room temperature powder X-ray patterns were recorded on PANalytical X'Pert-PRO powder X-ray diffractometer by means of $CuK\alpha_1$ radiation ($\lambda = 1.5406$ Å) in the angle range $10° \le 2\theta \le 110°$, with 10 s counting time for each step of 0.02° in order to determine the structure for all prepared ceramic compositions. Dielectric measurements were performed on ceramic discs by a Wayne-Kerr 6425 component analyzer after the deposition of gold electrodes on circular faces using cathodic sputtering. The temperature and frequency ranged between 250–575 K and 0.1– 200 kHz, respectively. The ferroelectric polarization (P–E) hysteresis measurements were recorded at room temperature using a ferroelectric test system (aix ACCT, TF Analyzer 1000). The Raman spectroscopy of the sintered samples was recorded in a backscattering configuration from 50 to 1000 cm^{-1} using a micro-Raman Horiba HR 800 spectrometer. The spectrometer had a wave number resolution of 3 cm^{-1} and was equipped with a microscope (Olympus BX41) with a Helium ion laser of 633 nm emission line with power of 15 mW and a CCD detector.

3. Results and discussions

3.1. Phase purity and microstructure

The XRD, at room temperature, was performed for all sintered samples. The obtained results indicated that our ceramic exhibits a single phase without impurity. The chemical elements in the different compositions were determined quantitatively using an EDX. This result confirmed the existence of desired elements, affirming the goodness of reactivity during synthesis (Fig. 1).

XRD patterns refinement was carried out for all compositions using the Fullprof program. All ceramics exhibit a tetragonal structure with space group *P4mm* and the indexation peak was carried out based on this space group. Fig. 2 shows profile-matching patterns of $Sr_{0.3}Na_{0.7}(Sn_{0.25}Ti_{0.75})_{0.3}Nb_{0.7}O_3$ ceramics, as example. Fig. 3 reveals the variations of the lattice parameters as well as the cell volume versus composition for $Na_{1-x}Sr_x$ $Sr_xNa_{1-x}(Sn_{0.25}Ti_{0.75x}Nb_{1-x}O_3$ (SNSTNx)) (x = 0.1, 0.2, 0.3 and 0.4) ceramics. These results indicate an increase of the lattice parameters in parallel with the composition x. This evolution could be attributed to the average radii in A, $\langle r_A \rangle$, and B, $\langle r_B \rangle$,

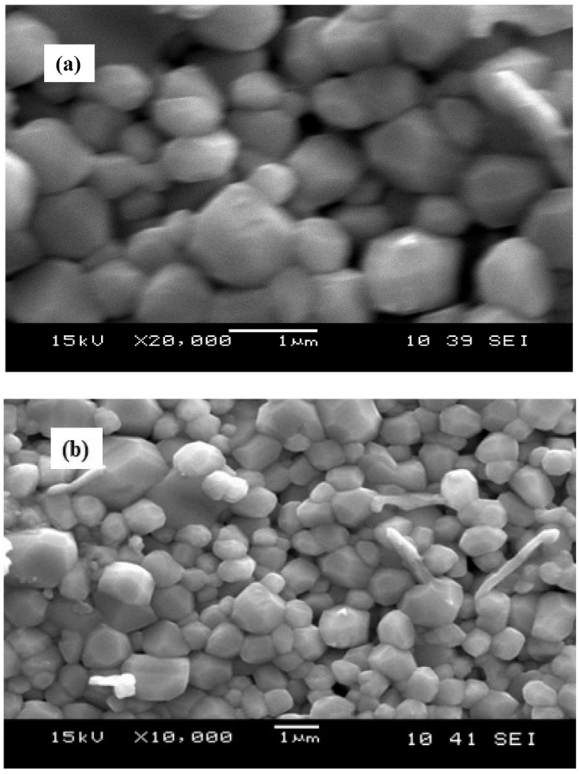

Fig. 1. SEM micrographs of the surface of $Na_{1-x}Sr_x(Sn_{0.25}Ti_{0.75})_xNb_{1-x}O_3$ ceramics **(a)** for x = 0.3 and **(b)** for x = 0.2 compositions.

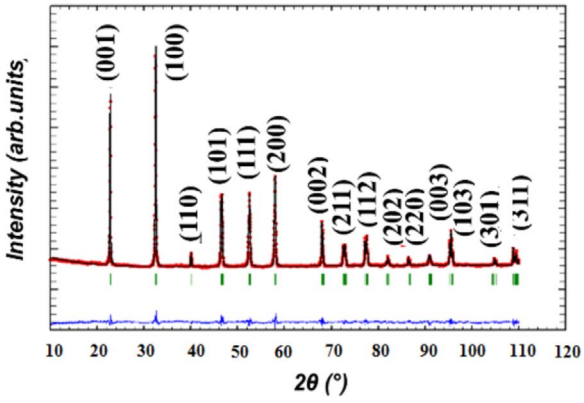

Fig. 2. Room temperature Profile-matching XRD patterns of $Na_{1-x}Sr_x(Sn_{0.25}Ti_{0.75})_xNb_{1-x}O_3$ ceramics with compositions x = 0.3.

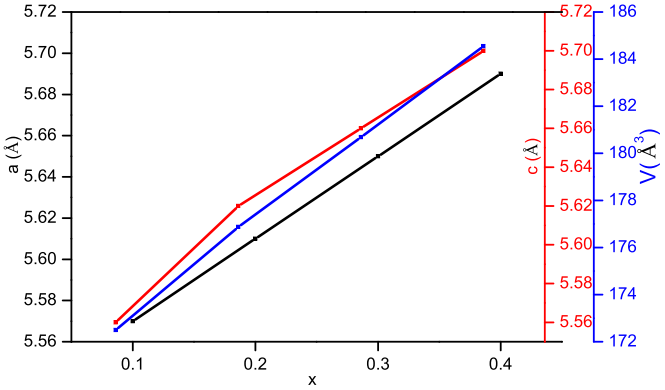

Fig. 3. Variations of the lattice parameters and cell volume versus compositions for $Na_{1-x}Sr_x(Sn_{0.25}Ti_{0.75})_xNb_{1-x}O_3$ ceramics.